

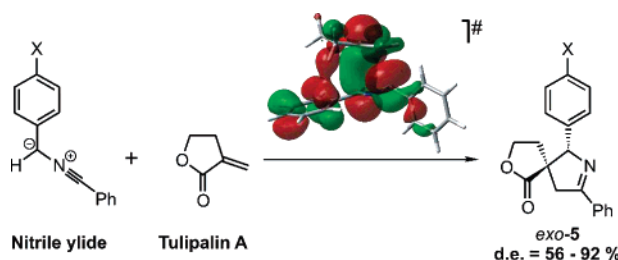
Substituent Effect on *exo* Stereoselectivity in the 1,3-Dipolar Cycloaddition Reaction of Tulipalin A with Nitrile Ylides

Petr Melša,[†] Michal Čajan,[‡] Zdeněk Havlas,[§] and Ctibor Mazal^{*,†}

Department of Chemistry, Faculty of Science, Masaryk University, Kotlářská 2, 611 37 Brno, Department of Inorganic Chemistry, Faculty of Science, Palacký University, Křížkovského 10, 771 47 Olomouc, and Institute of Organic Chemistry and Biochemistry, Academy of Sciences of the Czech Republic, Flemingovo nám. 2, 166 10 Prague 6, Czech Republic

mazal@chemi.muni.cz

Received November 29, 2007



1,3-Dipolar cycloaddition reactions of dihydro-3-methylene-2(3*H*)-furanone (tulipalin A) with various benzonitrile(*p*-*X*-benzylidene) ylides prefer formation of *exo*-cycloadducts in the extent corresponding to an increasing electron donor character of the substituent X in the *para*-position of the benzylidene phenyl ring of the 1,3-dipolar reagent. The substituent effect on diastereoselectivity of the 1,3-DC reaction is rationalized in terms of CH/ π interaction between the dipole and the dipolarophile in an *exo*-transition state. The determining role of such an interaction is demonstrated by the correlation of the observed diastereoselectivities with substituent Hammett σ constants, which shows a small negative ρ value. A certain contribution of CO/ π interaction between the lactone carbonyl and the substituted phenyl ring to mediation of the substituent effect is also discussed. The energy profiles of both reaction pathways were analyzed using DFT and RI-MP2 theoretical approaches. Calculated energy and structural differences between located transition states are consistent with reaction diastereoselectivities.

Introduction

1,3-Dipolar cycloaddition (1,3-DC) reactions have acquired a high reputation in the field of organic synthesis, becoming probably the most frequently used tool for construction of five-membered heterocycles. The popularity of this reaction benefits from the reaction mechanism concept based on frontier molecular orbital (FMO) theory that has been developing since the 1960s.¹ Using this theoretical approach and respecting the steric factors, chemists can make very reliable predictions of reactivity and regioselectivity in such reactions nowadays. On the other

hand, there is no general tool for the prediction of the stereochemical outcome of the cycloadditions in the cases where diastereoisomers can be formed as a result of different mutual orientations of the 1,3-dipolar reagent and dipolarophile in competing reaction transition states (TSs). To control the stereochemistry of these reactions, appropriate reagents are to be carefully chosen with respect to their various mutual interactions, which then result in a more or less preferred structure of the TS. Many factors affecting the energies of the possible TSs have to be usually considered in the process. Since even very small energy differences result in dramatic changes in the stereoisomer ratio, all the effects providing such energy contributions can play an important role. The unveiling and investigation of the effects that are worthy of such consideration is a continuous challenge.

Steric factors are obvious, proving to be of crucial importance in many cases.² In combination with metal coordination,³ they lie also in the ground of a vast majority of asymmetric versions

[†] Masaryk University.

[‡] Palacký University.

[§] Academy of Sciences of the Czech Republic.

(1) Padwa, A.; Pearson, W. H., Ed. *Synthetic Applications of 1,3-Dipolar Cycloaddition Chemistry Toward Heterocycles and Natural Products*; J. Wiley: New York, 2002. Padwa, A., Ed. *1,3-Dipolar Cycloaddition Chemistry*; J. Wiley: New York, 1984. Huisgen, R. *Angew. Chem.* **1963**, *75*, 604. Woodward, R. B.; Hoffmann, R. *J. Am. Chem. Soc.* **1965**, *87*, 395.

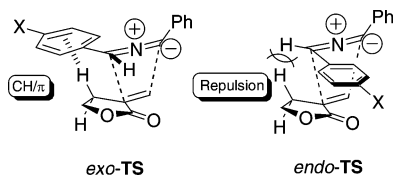


FIGURE 1. Supposed weak intermolecular interactions influencing *exo*- and *endo*-TS formation.

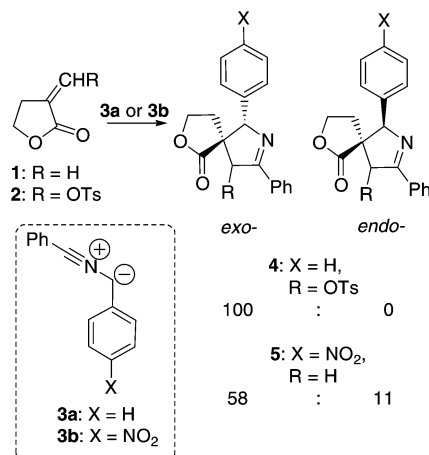
of such 1,3-DCs,⁴ where diastereoselective conditions are created with the assistance of chiral catalysts or auxiliaries. Additionally some other concepts have also been used to rationalize the stereochemistry of several 1,3-DC reactions. Secondary orbital interaction, for instance, worked well to explain diastereoselectivity of a nitron 1,3-DC to substituted styrenes.⁵ In a particular case of the latter reaction, an exceptional formation of a single diastereoisomer was ascribed to formation of a hydrogen bond between the dipole and the dipolarophile in the corresponding TS. A similar effect of a hydrogen bond was demonstrated in reactions of benzonitrile oxide with 4-(benzoylamino)cyclopent-2-enone.⁶ A hyperconjugative interaction along the acrylonitrile CN group and methylene hydrogen of an azomethine ylide 1,3-dipole was recognized to favor the *endo*-TS of the respective 1,3-DC reaction.⁷

In this paper, we demonstrate that also CH/ π interaction between the dipole and the dipolarophile could play an important role in preferential formation of either TS of a 1,3-DC reaction. Our results try to show that provided some structural prerequisites are present even such a weak intermolecular interaction as the CH/ π interaction has to be seriously taken into account in considerations of rationalizing reaction diastereoselectivity.

Results and Discussion

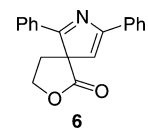
Effect of CH/ π Interaction on the Diastereoselectivity of 1,3-DC. Recently, we reported an example of outstanding diastereoselectivity in the 1,3-DC of a photochemically generated nitrile ylide to an α -methylene lactone derivative.⁸ Comparing our results with those obtained by de March et al. in analogous reactions,⁹ we suggested that CH/ π interaction¹⁰ could be very important in the evaluation of differences in the observed reaction diastereoselectivities. In our opinion, there are two main interactions in possible TSs (Figure 1), which can significantly affect the resulting *endo/exo* ratio, the CH/ π interaction in *exo*-TS, and hydrogen–hydrogen repulsion in *endo*-TS.

SCHEME 1. Nitrile Ylide **3a** Was Prepared from 2,3-Diphenyl-2*H*-azirine by UV Irradiation in Benzene (Method A)⁸ and **3b** from an Imidoyl Chloride by Reaction with TEA or *t*-BuOK in THF (Method B)⁹



The hydrogen–hydrogen repulsion disfavors the *endo*-TS in both cases, but seems to be hardly affected by substituents to such an extent that corresponds to the observed diastereoselectivity. On the contrary, the CH/ π interaction that would favor the *exo*-TS could be more sensitive to substituent effects. Unlike tulipalin A (**1**) used by de March, our methylene lactone derivative **2** was substituted at the exocyclic double bond with a tosyloxy group. The presence of such a strong electron-withdrawing substituent at the double bond increases the “acidic” character of the “allylic” C–H bond in the β position of the lactone ring, thus making the bond a more attractive candidate for possible CH/ π interaction. Also, the unsubstituted phenyl ring of 1,3-dipolar reagent **3a** that was used in our case is obviously a better π -electron donor. The combination of the stronger electron donor (better H-acceptor) with the better H-donor in the *exo*-TS implies then stronger CH/ π interaction between dipole **3a** and dipolarophile **2**. This results in exclusive formation of the *exo*-**4** diastereoisomer in our case, while de March isolated only a mixture of diastereoisomers **5** (Scheme 1).

To obtain closer insight into the reasons for reaction stereoselectivity, a cross-experiment was suggested at first. We tried to alternate the substrates and reagents of both reactions to combine the better H-donor with the poorer H-acceptor and *vice versa* and look at changes in the reaction diastereoselectivity. However, UV light used for generation of ylide **3a** from 2,3-diphenyl-2*H*-azirine⁸ (method A) in the reaction with **2** caused a fast polymerization of **1**. The reaction of **3b** with **2** was also unsuccessful, since the base necessary for thermal formation of nitrile ylide from imidoyl chloride⁹ (method B) eliminated tosylate from emerging the cycloadduct readily, yielding only a single product, **6**. Therefore, we were not able to determine a diastereoisomeric outcome of the reaction.



After this failure, we decided to study the cycloaddition of the methylene lactone **1** in more detail and, to verify our preliminary assumption about CH/ π interaction, to vary the

(2) For some illustrative examples of facial selectivity see: Melša, P.; Mazal, C. *Collect. Czech. Chem. Commun.* **2002**, *67*, 353. Dunstan, J. B. F.; Else, G. M.; Russell, R. A.; Savage, G. P.; Simpson, G. W.; Tiekink, E. R. T. *Aust. J. Chem.* **1998**, *51*, 499. Pereira, S. M.; Savage, G. P.; Simpson, G. W.; Greenwood, R. J.; Mackay, M. F. *Aust. J. Chem.* **1993**, *46*, 1401.

(3) Kamimura, A.; Kaneko, Y.; Ohta, A.; Matsuura, K.; Fujimoto, Y.; Kakehi, A.; Kanemasa, S. *Tetrahedron* **2002**, *58*, 9613.

(4) Gothelf, K. V. In *Cycloaddition Reactions in Organic Synthesis*, 1st ed.; Kobayashi, S., Jorgensen, K. A., Eds.; Wiley-VCH: Weinheim, Germany, 2002; Chapter 6, p 211.

(5) Chiacchio, U.; Casuscelli, F.; Corsaro, A.; Rescifina, A.; Romeo, G.; Uccella, N. *Tetrahedron* **1994**, *50*, 6671.

(6) Quadrelli, P.; Fassardi, V.; Cardarelli, A.; Caramella, P. *Eur. J. Org. Chem.* **2002**, 2058.

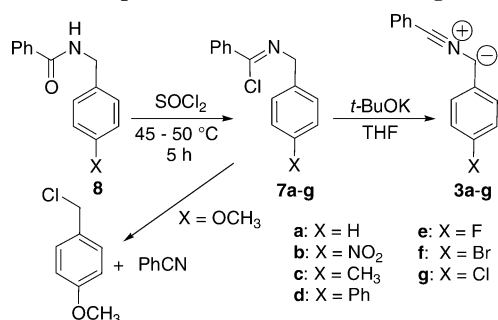
(7) Domingo, L. R. *J. Org. Chem.* **1999**, *64*, 3922.

(8) Častulík, J.; Jonas, J.; Mazal, C. *Collect. Czech. Chem. Commun.* **2000**, *65*, 708.

(9) de March, P.; el Arrad, M.; Figueredo, M.; Font, J. *Tetrahedron* **1998**, *54*, 11613.

(10) For a recent review about CH/ π hydrogen bonds in organic reactions see: Nishio, M. *Tetrahedron* **2005**, *61*, 6923.

SCHEME 2. Preparation of Nitrile Ylides 3a–g



substituents at the ylide reagent. We prepared *para*-substituted *N*-benzylbenzimidoyl chlorides **7a–g** from benzamides **8** and used the more flexible thermal method B to generate a set of substituted 1,3-dipolar reagents. The substituents were chosen with respect to their different electronic effects on the phenyl ring, which was expected to take part in the assumed CH/ π interaction. It must be noted here that imidoyl chlorides with strong electron-donating substituents, such as a methoxy group, were unstable and decomposed in the von Braun reaction¹¹ to benzonitrile and the corresponding substituted benzyl chlorides (Scheme 2). This limited the range of available substituents.

Ylides **3a–g** were added to methylene lactone **1**, and the diastereoisomer composition of the crude reaction mixtures was followed by ¹H NMR spectroscopy. Signals of methine group protons of the 1-pyrroline ring were indicative in diastereoisomer identification. Their chemical shifts differed by almost 0.2 ppm, ranging between 5.6 and 5.7 ppm for *exo-5* diastereoisomers and between 5.4 and 5.5 ppm for *endo-5*. We were able to confirm de March's conclusions about diastereoisomer configurations, which were based on NOESY of the minor stereoisomer *endo-5a*, by a successful X-ray structure analysis of *exo-5a*. (A corresponding CIF file and an ORTEP representation of the structure can be found in the Supporting Information). Minor diastereoisomers were not isolated from the reaction mixtures in most cases, but they undoubtedly possess the same constitution as the major ones as clearly evidenced by ¹H NMR spectra. For both diastereoisomers, the most downfield shifted signals ($\delta = 7.92\text{--}7.96$ ppm) were those of the *ortho*-protons of the unsubstituted phenyl ring. This was due to magnetic anisotropy of the adjacent C=N double bond, which unambiguously proves that the unsubstituted phenyl is always in position 8 of the spiroheterocyclic system. The regioisomers with the substituted phenyl ring in position 8 were not identified in the crude reaction mixtures. This means that the equilibrium between the relative regioisomers of nitrile ylides **3** described by Huisgen¹² and recently investigated also by others¹³ did not take place in our case appreciably.

According to our assumption about the important role of CH/ π interaction in the cycloaddition stereoselectivity, we expected that the amount of *exo*-adduct would increase with the electron donor ability of the substituent. Indeed, the *exo/endo*-diastereoisomer ratio in adducts **5a–g** increased in the order NO₂ < Cl < Br < F < Ph < H < CH₃ as obvious from Table 1.

(11) von Braun, J.; Müller, C. *Ber. Dtsch. Chem. Ges.* **1906**, *39*, 2018. Vaughan, W. R.; Carlson, R. D. *J. Am. Chem. Soc.* **1962**, *84*, 769.

(12) Huisgen, R.; Stangl, H.; Sturm, H. J.; Raab, R.; Bunge, K. *Chem. Ber.* **1972**, *105*, 1258. Bunge, K.; Huisgen, R.; Raab, R. *Chem. Ber.* **1972**, *105*, 1296.

(13) Yoo, C. L.; Olmstead, M. M.; Tantillo, D. J.; Kurth, M. J. *Tetrahedron Lett.* **2006**, *47*, 477.

TABLE 1. Results of Diastereoselective Cycloadditions of Nitrile Ylides 3a–g to Methylene Lactone 1

dipole 3 and product 5	X	<i>exo-5/endo-5</i> ^a	de ^a (%)	isolated yield of <i>exo-5</i> (%)
a	H	13.3	86	29
b	NO ₂	3.7 ^b	56	37
c	CH ₃	24	92	32
d	Ph	11.5	84	40
e	F	7.3	75	27
f	Br	6.7	73	29
g	Cl	5.7	70	22

^a Determined from ¹H NMR spectra of crude reaction mixtures. ^b The ratio 58/11 given in ref 9 came from isolated yields of **5b**.

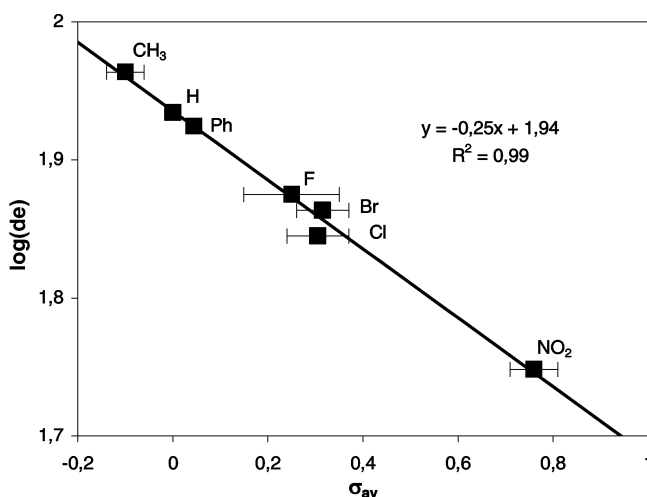


FIGURE 2. Linear fit of the log(de) vs σ_{av} plot. Error bars show intervals between σ_m and σ_p^0 values.

Hammert-like Plot of the Substituent Effect on Diastereoselectivity. Hammett correlation analysis is frequently used to evaluate substituent electronic effects on chemical reactions more precisely. We have found that diastereoisomer excesses of **5a–g** [log(de)] correlate with σ values of nitrile ylide substituents in a Hammett-like plot (Figure 2). A small negative ρ value (-0.250) shows that the electron donor substituents on the phenyl favor formation of *exo*-diastereoisomers. This is in good agreement with the concept of CH/ π interaction, where the more electron rich phenyl ring is subsequently a better H-acceptor. The interaction then decreases the energy of the corresponding *exo*-TS, thus increasing the amount of *exo*-cycloadduct in the reaction product. Since the intermolecular CH/ π interaction is difficult to localize with respect to the *para*- or *meta*-position toward the phenyl ring substituent, it is not surprising that acceptable correlations were found for both σ_p^0 and σ_m values¹⁴ ($R^2 = 0.96$ and $R^2 = 0.97$, respectively). In Figure 2, therefore, a plot of log(de) vs average σ values, $\sigma_{av} = (\sigma_p^0 + \sigma_m)/2$, is shown with error bars depicting the range ($\sigma_p^0 - \sigma_m$). We believe that the average σ values reflect the substituent effect on the electron donor character of the phenyl ring much better than the “simple” σ values, which were originally introduced to evaluate the effects of the substituents placed at a particular position of the phenyl ring on the reaction carried out at a side chain reaction center. Some other convenient representation of such a substituent effect, which would be more

(14) Exner, O. In *A Critical Compilation of Substituent Constants. In Correlation Analysis in Chemistry—Recent Advances*; Chapman, N., B., Shorter, J., Eds.; Plenum Press: New York, 1978; p 439.

TABLE 2. Energy, Structural, and Charge Distribution Comparison of TSs of the *exo* and *endo* Reaction Pathways to Products **5** Obtained by Used Methods of Calculation

product	B3LYP/aug-cc-pVDZ				MPW1K/aug-cc-pVDZ					RI-MP2/aug-cc-pVDZ			
	$\Delta\Delta E/\Delta\Delta G$ (kcal·mol ⁻¹)	interaction distance (Å)				$\Delta\Delta E/\Delta\Delta G$ (kcal·mol ⁻¹)	ΔS (cal·mol ⁻¹ ·K ⁻¹)	interaction distance (Å)				NBO charge H-1	$\Delta\Delta E$ (kcal·mol ⁻¹)
		<i>d</i> ₁	<i>d</i> ₂	<i>d</i> ₃ / <i>d</i> ₄	<i>d</i> ₅			<i>d</i> ₁	<i>d</i> ₂	<i>d</i> ₃ / <i>d</i> ₄	<i>d</i> ₅		
<i>exo</i> - 5a		2.273	2.900	2.888			146.55	2.312	2.849	2.762		0.260	
	2.52/1.82					2.96/2.80							3.73
<i>endo</i> - 5a		2.270	2.983	3.361	2.730		146.51	2.307	2.931	3.256	2.582	0.231	
<i>exo</i> - 5b		2.249	2.890	2.936			160.57	2.294	2.825	2.769		0.264	
	2.16/2.14					2.52/2.29							2.95
<i>endo</i> - 5b		2.256	2.954	3.309	2.753		160.82	2.299	2.902	3.200	2.634	0.236	
<i>exo</i> - 5c		2.278	2.902	2.913			156.19	2.318	2.850	2.779		0.259	
	2.36/2.13					2.87/2.53							3.92
<i>endo</i> - 5c		2.276	2.984	3.441	2.678		156.73	2.315	2.943	3.295	2.609	0.230	
<i>exo</i> - 5d		2.274	2.906	2.905			170.20	2.320	2.849	2.769		0.259	
	2.37/2.54					2.80/2.38							3.87
<i>endo</i> - 5d		2.267	2.999	3.358	2.708		171.01	2.307	2.956	3.233	2.625	0.231	
<i>exo</i> - 5e		2.277	2.894	2.924			150.88	2.318	2.844	2.791		0.260	
	2.16/2.03					2.61/2.39							3.28
<i>endo</i> - 5e		2.277	2.975	3.336	2.699		151.14	2.318	2.935	3.207	2.620	0.231	
<i>exo</i> - 5f		2.272	2.891	2.918			156.19	2.313	2.833	2.769		0.261	
	2.29/2.56					2.74/2.40							3.47
<i>endo</i> - 5f		2.272	2.971	3.327	2.715		156.79	2.312	2.922	3.208	2.609	0.232	
<i>exo</i> - 5g		2.271	2.897	2.933			154.34	2.314	2.842	2.777		0.261	
	2.29/2.14					2.73/2.61							3.37
<i>endo</i> - 5g		2.272	2.983	3.318	2.707		154.22	2.312	2.930	3.222	2.568	0.232	

correct but still at hand, can hardly be found otherwise. The plots with σ_p^0 and σ_m are available in the Supporting Information.

Theoretical Calculations. 1,3-DC reactions of methylene lactone **1** with nitrile ylides **2** were also investigated by theoretical calculations using *density functional theory* (DFT)¹⁵ with the B3LYP¹⁶ and MPW1K¹⁷ functionals and RI-MP2¹⁸ methods to locate TSs along the reaction pathways. DFT calculations were performed using the Gaussian03 program;¹⁹ RI-MP2 calculations were performed with the TURBOMOLE 5.6 program.²⁰ Geometries of the assumed structures were fully optimized using the Berny algorithm on both the B3LYP and MPW1K levels with the aug-cc-pVDZ basis set. Harmonic frequency analysis was used to verify their nature as the true TSs as well as for the calculation of zero-point vibrational energies. Each TS gave only one imaginary harmonic frequency corresponding to the motion involving formation of both new C–C bonds. Zero point energy (ZPE) corrections, enthalpies,

and entropies were calculated for 298.15 K and 101.325 kPa. Since the RI-MP2 optimization is still computationally very demanding, the geometries were optimized at the MPW1K/aug-cc-pVDZ level and only single-point energies were evaluated at the RI-MP2 level. The electron distribution in the TSs was analyzed using the *natural bond orbitals* (NBOs).²¹

Table 2 lists important geometrical parameters of calculated TS structures, which are obvious from the optimized geometry of the *exo*- and *endo*-TSs of **3b** with **1** shown in Figure 3. Activation electronic energy differences ($\Delta\Delta E$) and activation free energy differences ($\Delta\Delta G$) calculated as differences between the corresponding energies of *endo*- and *exo*-TSs are also summarized in Table 2. The ΔE and ΔG energies, entropy (ΔS), and imaginary frequencies (ν_{img}) of the transition states are available in the Supporting Information.

In general, the process of C•••C bonds forming is similar for both *exo*- and *endo*-TSs in all the reactions. The significant difference in the lengths of the bonds formed in each of the found TSs (Table 2) indicates an asynchronous reaction mechanism. The activation energies of the *exo* reaction pathways are lower in all the studied cases (Table 2). Similarly to the experimental results, preference of the *exo* reaction pathway is more significant for ylides substituted by more electron donor groups.

Hydrogen–hydrogen repulsion (see Figures 1 and 3 and *d*₅ in Table 2) undoubtedly is unfavorable to the process of *endo*-TS formation. It is assumed that the extent of this effect will rather be independent of substitution at the ylide phenyl ring. This expectation well corresponds with calculated structural parameters of each individual case of *endo*-TSs (for details, see values *d*₁ and *d*₂ in Table 2). Similarly, NBO analysis provided almost equal values of partial charge on H-1 atoms for all studied cases (Table 2).

On the contrary, two weak attractive interactions come forward in the *exo*-TS according to its spatial arrangement: a

(15) Hohenberg, P.; Kohn, W. *Phys. Rev. B* **1964**, *136*, 864.

(16) Lee, C.; Yang, W.; Parr, R. G. *Phys. Rev. B* **1988**, *37*, 785.

(17) Lynch, B. J.; Fast, P. L.; Harris, M.; Truhlar, D. G. *J. Phys. Chem. A* **2000**, *104*, 4811.

(18) Feyereisen, M.; Fitzgerald, G.; Komornicky, A. *Chem. Phys. Lett.* **1993**, *208*, 359.

(19) Frisch, M. J.; Trucks, G. W.; Schlegel, H. B.; Scuseria, G. E.; Robb, M. A.; Cheeseman, J. R.; Montgomery, J. A., Jr.; Vreven, T.; Kudin, K. N.; Burant, J. C.; Millam, J. M.; Iyengar, S. S.; Tomasi, J.; Barone, V.; Mennucci, B.; Cossi, M.; Scalmani, G.; Rega, N.; Petersson, G. A.; Nakatsuji, H.; Hada, M.; Ehara, M.; Toyota, K.; Fukuda, R.; Hasegawa, J.; Ishida, M.; Nakajima, T.; Honda, Y.; Kitao, O.; Nakai, H.; Klene, M.; Li, X.; Knox, J. E.; Hratchian, H. P.; Cross, J. B.; Bakken, V.; Adamo, C.; Jaramillo, J.; Gomperts, R.; Stratmann, R. E.; Yazyev, O.; Austin, A. J.; Cammi, R.; Pomelli, C.; Ochterski, J. W.; Ayala, P. Y.; Morokuma, K.; Voth, G. A.; Salvador, P.; Dannenberg, J. J.; Zakrzewski, V. G.; Dapprich, S.; Daniels, A. D.; Strain, M. C.; Farkas, O.; Malick, D. K.; Rabuck, A. D.; Raghavachari, K.; Foresman, J. B.; Ortiz, J. V.; Cui, Q.; Baboul, A. G.; Clifford, S.; Cioslowski, J.; Stefanov, B. B.; Liu, G.; Liashenko, A.; Piskorz, P.; Komaromi, I.; Martin, R. L.; Fox, D. J.; Keith, T.; Al-Laham, M. A.; Peng, C. Y.; Nanayakkara, A.; Challacombe, M.; Gill, P. M. W.; Johnson, B.; Chen, W.; Wong, M. W.; Gonzalez, C.; and Pople, J. A. *Gaussian 03*, Revision C.02; Gaussian, Inc.: Wallingford, CT, 2004.

(20) Ahlrichs, R.; Bär, M.; Häser, M.; Horn, H.; Kölmel, C. *Chem. Phys. Lett.* **1989**, *162*, 165.

(21) Reed, A. E.; Curtiss, L. A.; Weinhold, F. *Chem. Rev.* **1988**, 899.

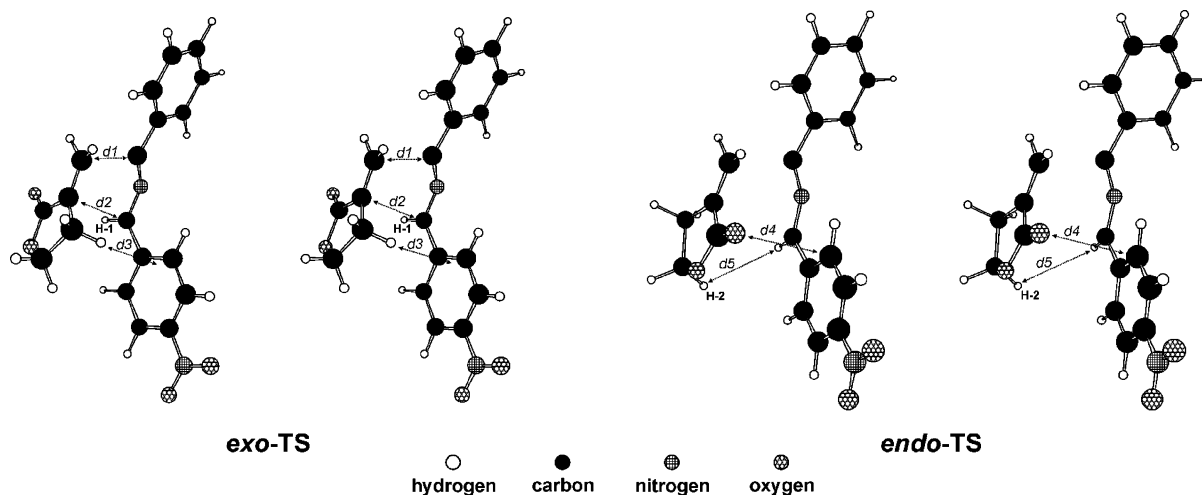


FIGURE 3. Stereoview of calculated structures of the *exo*-TS and *endo*-TS of 1,3-DC reaction of **3b** and lactone **1**.

CH/ π interaction between the substituted phenyl ring of the nitrile ylide and the β -hydrogen atom of the lactone ring and a dipole–dipole-like Coulombic interaction between the ylide C–H bond and the lactone carbonyl bond. As for the CH/ π interaction, calculated distances between the ylide phenyl ring and the β -hydrogen atom are about 2.90 and 2.77 Å for the B3LYP and MPW1K calculations, respectively (Table 2, Figure 3). This is a prerequisite for the expected CH/ π interaction. As for the Coulombic interaction, the more electron withdrawing substituent could possibly increase the positive charge of the C–H bond hydrogen, thus strengthening the attractive interaction with the lactone carbonyl. This would affect the reaction stereoselectivity unlike the observed substituent effect, and hence, the contribution of the Coulombic interaction, if any, would be evidently lower than that of CH/ π interaction. Moreover, an inspection of calculated H-1 charges (Table 2) did not reveal significant changes due to substitution.

Geometries found for *endo*-TSs show an additional close contact. Interatomic distances (d_4) between the oxygen atom of the lactone carbonyl and the carbon in the *meta*-position of the nitrile ylide phenyl range between 3.295 and 3.200 Å for methyl- and nitro-substituted ylides, respectively (Table 2). The phenomenon of noncovalent interaction between a carbonyl and various π -systems (CO/ π interaction) currently attracts the attention of structural chemists and theoreticians, becoming evident for instance from searches of structural patterns of nucleic acids and proteins in the Cambridge Structural Database²² as well as from other observations.²³ The concept of CO/ π interaction has also been used to explain an enhanced selectivity in separation of aromatic analytes on some HPLC stationary phases.²⁴ Recent results²² show that the CO/ π interaction can be expected also for groups in such mutual orientation as that found in our *endo*-TSs. CO/ π interaction can be energetically favorable for the electron-deficient phenyl ring but will decrease or disappear with increasing electron density of the aromatic π -system. This means that the substituent effect on reaction diastereoselectivity mediated by this kind of interaction will

show a tendency similar to that due to the CH/ π interaction, favoring formation of *endo*-adducts for electron-withdrawing substituents.

Since the effect of even the most electron withdrawing substituent, the nitro group, where a maximum CO/ π contribution and a minimum CH/ π contribution can be expected, did not result in an excess of the *endo*-diastereoisomer, the main reaction preference for the *exo* pathway originates most probably for the steric reasons. The actual diastereoisomer ratio formed in a particular reaction is the result of modification of this main steric preference by the other effects, among which the weight of the CH/ π interaction is evident.

In light of the recent view on the nature and origin of CH/ π interaction, which reveals a dominant contribution of dispersion interaction²⁵ in the case of nonactivated C–H bonds, it is interesting that analysis of the TS's molecular orbitals shows a certain delocalization of electron density in the *exo*-TS's HOMO across the C–H bond pointing to the phenyl ring (Figure 4). Slightly weaker delocalization is discernible also at the lobe of the C=O bond π -orbital facing the phenyl ring in the *endo*-TS's HOMO.

Concerning quantitative description of the reaction pathway energy profiles, we have compared the more frequently used B3LYP hybrid functional with the MPW1K functional that was designed just for TS structures and activation barrier predictions.^{17,26,27} The B3LYP approach underestimates the results by approximately 0.3 kcal.mol⁻¹, in comparison with those obtained by the MPW1K functional with the same basis set. In general, both functionals provide the activation energy differences ($\Delta\Delta E$, $\Delta\Delta G$), which roughly correlate with the observed diastereoselectivity (lower stereoselectivity for strong electron-withdrawing substituents), but they fail to reflect relatively small differences such as those between hydrogen and the methyl substituent (see Table 2 and Figure 5). As density functional theory does not exactly describe the electron correlation and weak interactions, the energies of the located TSs have also been calculated at the

(22) Egli, M.; Sarkhel, S. *Acc. Chem. Res.* **2007**, *40*, 197.

(23) Gautrot, J. E.; Hodge, P.; Cupertino, D.; Helliwell, M. *New J. Chem.* **2006**, *30*, 1801.

(24) Rahman, M. M.; Takafuji, M.; Ihara, I. *J. Chromatogr. A* **2006**, *1119*, 105. Rahman, M. M.; Takafuji, M.; Ansarian, H. R.; Ihara I. *Anal. Chem.* **2005**, *77*, 6671. Goto, Y.; Nakashima, K.; Mitsuishi, K.; Takafuji, M.; Sakaki, S.; Ihara, H. *Chromatographia* **2002**, *56*, 19.

(25) Shibasaki, K.; Fujii, A.; Mikami, N.; Tsuzuki, S. *J. Phys. Chem. A* **2006**, *110*, 4397. Tsuzuki, S.; Honda, K.; Uchimar, T.; Mikami, M.; Fujii, A. *J. Phys. Chem. A* **2006**, *110*, 10163. Morita, S.; Fujii, A.; Mikami, N.; Tsuzuki, S. *J. Phys. Chem. A* **2006**, *110*, 10583. Shibasaki, K.; Fujii, A.; Mikami, N.; Tsuzuki, S. *J. Phys. Chem. A* **2007**, *111*, 753.

(26) Parthiban, S.; de Oliveira, G.; Martin, J. M. L. *J. Phys. Chem. A* **2001**, *105*, 895.

(27) Ess, D. H.; Houk, K. N. *J. Phys. Chem. A* **2005**, *109*, 9542.

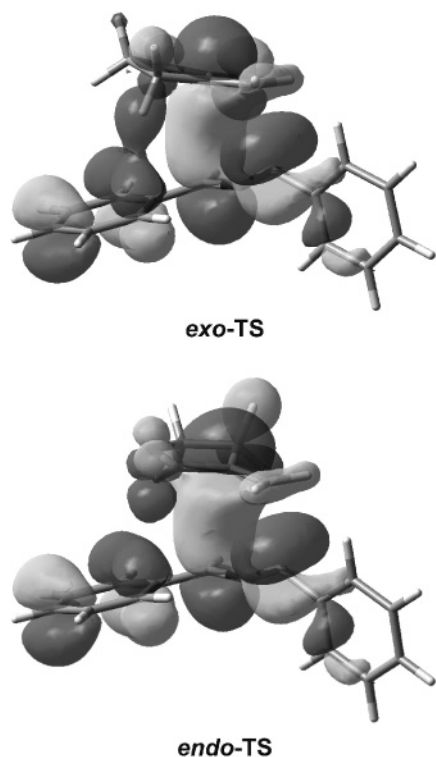


FIGURE 4. TS structures of the *exo* and *endo* reaction pathways: graphical representation of the HOMOs.

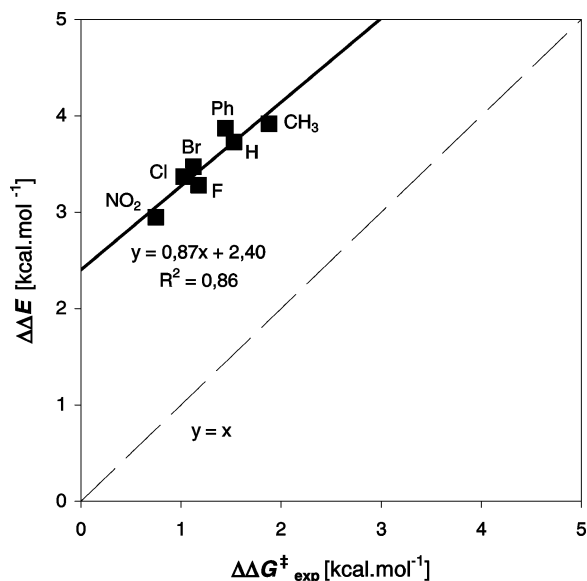


FIGURE 5. Correlation of $\Delta\Delta G_{\text{exp}}^{\ddagger}$ free energy differences obtained from experimentally determined diastereoisomer ratios (*exo*-5/*endo*-5) and $\Delta\Delta E$ electronic energy differences calculated by RI-MP2/aug-cc-pVDZ.

RI-MP2 level of theory. The RI-MP2 approach differs from the standard MP2 perturbation method in the treatment of Coulomb integrals. These integrals are calculated with the projected wave function on a smaller particularly optimized basis set, which speeds the calculation enormously while introducing only small error.^{28,29,30} Since the MPW1K hybrid functional predicts quite

(28) Weigend, F.; Häser, M.; Patzelt, H.; Ahlrichs, R. *Chem. Phys. Lett.* **1998**, *294*, 143.

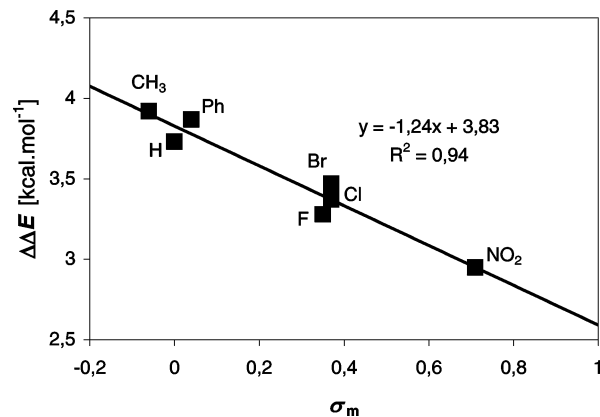


FIGURE 6. Hammett plot correlating electronic energy differences $\Delta\Delta E$ calculated by RI-MP2/aug-cc-pVDZ and substituent σ_m constants.

accurate saddle point geometries,¹⁷ we have used data obtained on this level. Calculated RI-MP2/aug-cc-pVDZ $\Delta\Delta E$ energy differences correlate with experimental observations much better than those of both DFT methods (compare the results in Tables 1 and 2, respectively).

To compare our calculations with the experimental values, the energy RI-MP2 differences $\Delta\Delta E$ were correlated with $\Delta\Delta G_{\text{exp}}^{\ddagger}$ determined from experimentally obtained diastereoisomer ratios in a plot depicted in Figure 5. The correlation clearly shows that the calculated values well follow the substitution effect observed in experiment, albeit the calculations systematically overvalue the energy differences by approximately $2.4 \text{ kcal}\cdot\text{mol}^{-1}$. Since the entropy contributions to the ΔG^{\ddagger} values calculated by DFT are almost identical for corresponding pairs of *endo*- and *exo*-TSs (see Table 2), the $\Delta\Delta E$ values should be equal to the $\Delta\Delta G^{\ddagger}$ values. We can also justifiably assume that the RI-MP2 approach in principle should provide analogous results, so the systematic discrepancy is probably caused by an overestimation of the weak interactions by the methods used. On the other hand, an acceptable fit ($R^2 = 0.94$) that was found also for the Hammett-like plot of the $\Delta\Delta E$ differences with σ_m values could further evidence that the computational approach reflects the substituent effect satisfactorily well (Figure 6). It is correct to admit that the fit of σ_p^0 is of lower quality ($R^2 = 0.81$).

We are aware of accuracy limits of the computational methods used, which fall within $1\text{--}2 \text{ kcal}\cdot\text{mol}^{-1}$ according to the literature,³¹ thus being comparable to the energy differences obtained. However, it is obvious that the compared TSs do not differ much in their structures, so the error in the energy calculation should be of similar value, particularly for the same kind of diastereoisomers. Therefore, the relative energies of diastereoisomeric TSs, which reflect also the substitution effect, are supposed to be reasonable. The quality of the correlation with experimental data and the σ constants gives a good reasoning for such a conclusion.

(29) Jurečka, P.; Nachtigall, P.; Hobza, P. *Phys. Chem. Chem. Phys.* **2001**, *3*, 4578.

(30) Braun, J.; Neusser, H. J.; Hobza, P. *J. Phys. Chem. A* **2003**, *107*, 3918.

(31) Jones, G. O.; Ess, D. H.; Houk, K. N. *Helv. Chim. Acta* **2005**, *88*, 1702. Lynch, B. J.; Truhlar, D. G. *J. Phys. Chem. A* **2001**, *105*, 2936.

Conclusions

The reported 1,3-DC reaction of tulipalin A with nitrile ylides is an example of diastereoselective 1,3-DC reaction whose selectivity is significantly affected by CH/ π interaction. This weak attractive interaction between the lactone C(β)-H bond and the nitrile ylide phenyl ring, which significantly modifies the main tendency of the reaction to prefer the *exo* reaction pathway due to steric reasons, is demonstrated by a remarkable substituent effect correlating the observed diastereoselectivity with the phenyl substituent σ values in a Hammett-like plot. The low negative ρ value of the plot shows that electron donor substituents favor formation of *exo*-diastereoisomers. The results of DFT and mainly RI-MP2 computational analyses of the structures and properties of the possible TSs support this conclusion as well. The calculated geometries of the *exo*-TSs show that the considered β -hydrogen is close enough to interact with the nitrile ylide phenyl ring (approximately 2.9 Å). Moreover, the mutual orientation of the lactone carbonyl and the substituted phenyl ring of the ylide allows speculation also about some contribution of CO/ π interaction to the energy of the *endo*-TSs, which would exhibit a similar effect of the substituent. Evaluation of relative contributions of both interactions to mediation of the substituent effect on reaction stereoselectivity is, however, difficult due to computational demands. Our results show that the weak attractive interactions such as CH/ π and CO/ π interaction should also be taken into account among the effects capable of significantly affecting the diastereoselectivity of 1,3-DC reactions. We believe that further examples of such effects will appear soon.

Experimental Section

General Procedure for Cycloaddition Reaction of Nitrile Ylides to Tulipalin A. A solution of *t*-BuOK (315 mg, 2.66 mmol) in dry THF (10 mL) was added dropwise to a mixture of tulipalin A (200 mg, 2 mmol) and imidoyl chloride (2.66 mmol) in dry THF (2 mL) over a period of 4 h, and the reaction mixture was stirred overnight. After concentration on a rotary evaporator, the residue was redissolved in methylene chloride (30 mL), washed with water (50 mL), and dried over Na₂SO₄. The solvent was removed in vacuo, and the residue was subjected to column chromatography on silica gel using an ethyl acetate/benzene/hexane mixture (1:1:1) as the eluent to give the *exo*-cycloadduct as a clear oily liquid.

Data for (5*S,6*S**)-6,8-diphenyl-2-oxa-7-azaspiro[4.4]non-7-en-1-one (*exo*-5a):** yield 0.165 g, 29%; ¹H NMR (300 MHz, CDCl₃) δ 7.91 (d, J = 6.24 Hz, 2H), 7.50–7.43 (m, 3H), 7.37–7.30 (m, 5H), 5.63 (s, 1H), 4.09–4.01 (m, 1H), 3.67–3.57 (m, 2H), 3.26 (d, J = 16.63 Hz, 1H), 2.03–1.94 (m, 1H), 1.88–1.79 (m, 1H); ¹³C NMR (75 MHz, CDCl₃) δ 180.8, 171.3, 138.6, 133.6, 131.4, 128.8, 128.2, 128.0, 127.5, 81.4, 66.0, 54.1, 48.3, 32.3; IR (KBr) 3029, 2985, 2914, 1765, 1620, 1344, 1178, 1022, 761, 708 cm⁻¹; MS m/z (rel intens) 291 (M, 15), 246 (19), 193 (100), 165 (12), 90 (10), 89 (10); HRMS (ESI) m/z calcd for C₁₉H₁₄NO₂ (M - H₂ - 1) 288.1025, found 288.1034.

Data for (5*S,6*S**)-6-(4-nitrophenyl)-8-phenyl-2-oxa-7-azaspiro[4.4]non-7-en-1-one (*exo*-5b):** yield 0.246 g, 37%; ¹H NMR (300 MHz, CDCl₃) δ 8.24 (d, J = 8.7 Hz, 2H), 7.90 (d, J = 6.5 Hz, 2H), 7.53–7.45 (m, 5H), 5.73 (s, 1H), 4.18–4.10 (m, J = 7.4 Hz, 1H), 3.84–3.77 (m, 1H), 3.62 (dd, J = 16.6, 2.4 Hz, 1H), 3.36 (dd, J = 16.6, 1.01 Hz, 1H), 1.90–1.75 (m, 1H).

Data for (5*S,6*S**)-6-(4-methylphenyl)-8-phenyl-2-oxa-7-azaspiro[4.4]non-7-en-1-one (*exo*-5c):** yield 0.195 g, 32%; ¹H NMR (300 MHz, CDCl₃) δ 7.92–7.90 (dd, J = 2.0, 7.6 Hz, 2H), 7.49–7.42 (m, 3H), 7.21–7.15 (m, 4H), 5.60 (s, 1H), 4.09–4.01 (ddd, J = 1.0, 5.7, 8.0 Hz, 1H), 3.66–3.60 (dd, J = 2.4, 16.7 Hz,

1H), 3.66–3.57 (m, 1H), 3.28–3.22 (dd, J = 1.5, 16.7 Hz, 1H), 2.36 (s, 3H), 2.05–1.96 (ddd, J = 2.0, 5.8, 13.3 Hz, 1H), 1.87–1.78 (ddd, J = 1.2, 6.7, 13.2 Hz, 1H); ¹³C NMR (75 MHz, CDCl₃) δ 180.9, 171.1, 137.8, 135.4, 133.6, 131.2, 129.5, 128.8, 128.0, 127.3, 81.3, 66.0, 54.0, 48.2, 32.3, 21.2; IR (KBr) 3027, 2983, 2918, 1763, 1620, 1448, 1171, 1026, 764, 694 cm⁻¹; MS (EI) m/z (rel intens) 305 (M, 43), 259 (19), 207 (100), 104 (14), 78 (20); HRMS (ESI) m/z calcd for C₂₀H₁₆NO₂ (M - H₂ - 1) 302.1181, found 302.1195.

Data for (5*S,6*S**)-6-(4-phenylphenyl)-8-phenyl-2-oxa-7-azaspiro[4.4]non-7-en-1-one (*exo*-5d):** yield 0.293 g, 40%; ¹H NMR (300 MHz, CDCl₃) δ 7.95–7.93 (dd, J = 8.0, 1.9 Hz, 2H), 7.64–7.60 (m, 4H), 7.52–7.34 (m, 8H), 5.69 (s, 1H), 4.14–4.07 (dt, J = 8.0, 2.0 Hz, 1H), 3.74–3.65 (m, 2H), 3.33–3.28 (dd, J = 16.7, 1.2 Hz), 2.12–2.04 (dt, J = 13.4, 1.7 Hz, 1H), 2.12–1.84 (m, 1H); ¹³C NMR (75 MHz, CDCl₃) δ 180.9, 171.3, 141.1, 140.7, 137.6, 133.6, 131.5, 129.0, 128.9, 128.1, 128.0, 127.7, 127.5, 127.2, 81.2, 66.2, 54.1, 48.4, 32.4; IR (KBr) 3027, 2983, 2917, 1763, 1620, 1487, 1171, 1026, 764, 694 cm⁻¹; MS (EI) m/z (rel intens) 367 (M, 38), 322 (32), 269 (100), 165 (41), 78 (8); HRMS (ESI) m/z calcd for C₂₅H₁₈NO₂ (M - H₂ - 1) 364.1338, found 364.1351.

Data for (5*S,6*S**)-6-(4-Fluorophenyl)-8-phenyl-2-oxa-7-azaspiro[4.4]non-7-en-1-one (*exo*-5e):** yield 0.185 g, 27%; ¹H NMR (300 MHz, CDCl₃) δ 7.89 (dd, J = 8.1, 1.6 Hz, 2H), 7.50–7.42 (m, 3H), 7.31–7.26 (m, 2H), 7.06 (t, J = 8.6 Hz, 2H), 5.60 (s, 1H), 4.11–4.04 (ddd, J = 7.8, 1.4, 1.3 Hz, 1H), 3.69–3.58 (m, 2H), 3.30–3.24 (dd, J = 16.6, 1.1 Hz, 1H), 1.96–1.76 (m, 2H); ¹³C NMR (75 MHz, CDCl₃) δ 180.6, 171.4, 162.7 (d, J = 246.7 Hz), 134.4 (d, J = 3.2 Hz), 133.4, 131.5, 129.1 (d, J = 8.0 Hz), 128.9, 128.0, 115.8 (d, J = 21.6 Hz), 80.6, 66.0, 54.1, 48.3, 32.2; IR (KBr) 3074, 2989, 2919, 2863, 1759, 1608, 1510, 1226, 1174, 1024, 850, 782, 698, 563, 542 cm⁻¹; MS (EI) m/z (rel intens) 309 (M, 17), 263 (12), 211 (10), 107 (20); HRMS (ESI) m/z calcd for C₁₉H₁₃FNO₂ (M - H₂ - 1) 306.0930, found 306.0929.

Data for (5*S,6*S**)-6-(4-bromophenyl)-8-phenyl-2-oxa-7-azaspiro[4.4]non-7-en-1-one (*exo*-5f):** yield 0.215 g, 29%; ¹H NMR (300 MHz, CDCl₃) δ 7.92–7.88 (dd, J = 1.4, 8.2 Hz, 2H), 7.52 (d, J = 8.48 Hz, 2H), 7.53–7.43 (m, 3H), 7.21 (d, J = 8.4 Hz, 2H), 5.60 (s, 1H), 4.14–4.06 (ddd, J = 1.3, 1.5, 6.4 Hz, 1H), 3.74–3.66 (ddd, J = 1.4, 1.7, 6.1 Hz, 1H), 3.66–3.60 (dd, J = 2.2, 14.2 Hz, 1H), 3.32–3.26 (dd, J = 1.4, 16.7 Hz, 1H), 1.98–1.78 (m, 2H); ¹³C NMR (75 MHz, CDCl₃) δ 180.8, 171.9, 137.9, 133.6, 132.3, 131.8, 129.5, 129.1, 128.2, 122.4, 80.7, 66.3, 54.3, 48.6, 32.3; IR (KBr) 3060, 2917, 2864, 1765, 1622, 1487, 1169, 1026, 760, 694 cm⁻¹; MS (EI) m/z (rel intens) 305 (M), 369 (M, 16), 324 (142), 273 (100), 227 (58), 192 (93), 165 (20), 89 (59); HRMS (ESI) m/z calcd for C₁₉H₁₃BrNO₂ (M - H₂ - 1) 366.0130, found 366.0130.

Data for (5*S,6*S**)-6-(4-Chlorophenyl)-8-phenyl-2-oxa-7-azaspiro[4.4]non-7-en-1-one (*exo*-5g):** yield 0.145 g, 22%; ¹H NMR (300 MHz, CDCl₃) δ 7.89 (d, J = 8.0 Hz, 2H), 7.49–7.41 (m, 3H), 7.35 (d, J = 8.4 Hz, 2H), 7.25 (d, J = 8.4 Hz, 2H), 5.59 (s, 1H), 4.12–4.04 (m, 1H), 3.72–3.64 (m, 1H), 3.63–3.57 (dd, J = 16.6, 2.3 Hz, 1H), 3.30–3.24 (dd, J = 16.7, 0.9 Hz, 1H), 1.96–1.76 (m, 2H); ¹³C NMR (75 MHz, CDCl₃) δ 180.5, 171.5, 137.1, 134.0, 133.4, 131.6, 129.0, 128.9, 128.3, 128.0, 80.6, 66.0, 54.1, 48.3, 32.1; IR (KBr) 3060, 2918, 1766, 1618, 1491, 1171, 1026, 760, 692 cm⁻¹; MS (EI) m/z (rel intens) 324 (M - 1, 17), 279 (19), 227 (100), 191 (43), 89 (51); HRMS (ESI) m/z calcd for C₁₉H₁₃ClNO₂ (M - H₂ - 1) 322.0635, found 322.0637.

Acknowledgment. We thank the Academic Supercomputer Center at Masaryk University for providing us with access to the computer facilities and the Ministry of Education, Youth and Sports of the Czech Republic for financial support (Grant Nos. 570/2004, MSM6198959218, and LC512). We are grateful to Jiří Matoušek from the National Centre for Biomolecular Research at Masaryk University in Brno for giving us assistance

with performing the quantum chemistry calculations and to Dr. Ondřej Novák from the Laboratory of Growth Regulators at Palacký University in Olomouc for HR-MS measurements.

Supporting Information Available: Details of the experimental procedures and general methods of preparation of benzamides **8a–g** and imidoyl chlorides **7a–g**, NMR spectra of adducts **5a–g**,

additional Hammett-like plots, CIF file, and ORTEP picture of *exo*-**5a**, and Cartesian coordinates, energies, and imaginary frequencies of the TS structures optimized by the MPW1K/aug-cc-pVDZ method. This material is available free of charge via the Internet at <http://pubs.acs.org>.

JO702563N